issn 0065-3713

INSTITUT D'AERONOMIE SPATIALE DE BELGIQUE

3 - Avenue Circulaire
B - 1180 BRUXELLES

AERONOMICA ACTA

A - N° 399 - 1996

MOTION AND EROSION OF THE NIGHT SIDE PLASMAPAUSE REGION AND OF THE ASSOCIATED SUBAURORAL ELECTRON TEMPERATURE ENHANCEMENT : COSMOS-900 OBSERVATIONS

by

V.V. AFONIN, V.S. BASSOLO, J. SMILAUER and J. LEMAIRE

BELGISCH INSTITUUT VOOR RUIMTE-AERONOMIE

3 - Ringlaan
B - 1180 BRUSSEL

FOREWORD

This article has been accepted for publication in the special issue of Journal of Geophysical Research, dedicated to the memory of K. Gringauz (IKI, Moscow).

AVANT-PROPOS

Cet article a été accepté pour publication dans le numéro spécial de Journal of Geophysical Research dédié à la mémoire de K. Gringauz (IKI, Moscou).

VOORWOORD

Dit artikel is aanvaard voor publicatie in het speciale nummer van Journal of Geophysical Research ten aandenken aan K. Gringauz (IKI, Moskou).

VORWORT

Dieser Artikel wurde zur Veröffentlichung in der dem Angedenken von K. Gringauz (IKI, Moskau) gewidmeten Auflage des "Journal of Geophysical Research" angenommen.

MOTION AND EROSION OF THE NIGHT SIDE PLASMAPAUSE REGION AND OF THE ASSOCIATED SUBAURORAL ELECTRON TEMPERATURE ENHANCEMENT : COSMOS-900 OBSERVATIONS

by

V.V. AFONIN, V.S. BASSOLO, J. SMILAUER and J. LEMAIRE

Abstract

Ion densities, N_i and electron temperatures T_e measured onboard COSMOS-900 satellite (launched at March 30, 1977 into near polar circular orbit : i = 83°, h = 500 km, orbital period = 94 min) are used to study the behaviour of the ionosphere during the prestorm, initial and main phases of the magnetic storm of 1-2 Dec., 1977. The spatial resolution of the measurement was ≤ 0.3 degree latitude for T_e and ≤ 0.1 degree latitude for N_i. During this period 27 orbits were recorded in the onboard large storage memory. This enabled detailed study of the positions and latitude profiles of midlatitude ionospheric trough and subauroral electron temperature enhancement (SETE) in the midnight local time sector. Simultaneous proton density data measured on the high altitude satellites "PROGNOZ-5" and "PROGNOZ-6" confirm that the poleward boundary of the T_e peak corresponds to the ionospheric magnetic field projection of the high altitude plasmapause density "knee".

During the main phase of a geomagnetic storm the polar edge of the SETE becomes very steep. It coincides with an equally steep poleward edge of the midlatitude ionospheric trough, and, with the position of the newly forming density gradient of the high altitude plasmapause.

The sequence of COSMOS-900 observations clearly shows how the night-time midlatitude ionospheric trough fills up, as well as, how the subauroral electron temperature enhancement and the outer layers of the plasmasphere are eroded during a geomagnetic storm. These results shed new light on the of formation of the plasmapause in the post midnight sector and on the time dependent electric field distribution in the nightside sector before and during a geomagnetic storm.

Résumé

L'évolution de l'ionosphère supérieure lors de l'orage géomagnétique du 1-2 décembre 1977, a été étudiée avec les observations de la densité ionique, N_i, la température électronique, Te, mesurées à l'aide du satellite COSMOS-900, lancé le 30 mars 1977, sur une orbite polaire d'inclinaison i = 83°, d'altitude h = 500 km et de période orbitale de 94 minutes. La résolution spatiale des mesures satellitaires est ≤ 0.3 degré de latitude pour T_e, et ≤ 0.1 degré de latitude pour N_i. Les observations étaient enregistrées à bord dans des mémoires à grande capacité. La période d'observation couvrant 27 orbites consécutives a permis d'étudier en détail l'évolution de la position et du profil de la distribution de densité et de température dans la région subaurorale nocturne où l'on observe un pic de température électronique (SETE, Subauroral Electron Temperature Enhancement). Des observations simultanées de la densité ionique à haute altitude avec le satellite PROGNOZ-5 et PROGNOZ-6 confirment que le gradient de densité formant la plasmapause (à haute altitude) se projecte dans l'ionosphère à l'endroit où se trouve le bord polaire du SETE.

Pendant la phase principale de l'orage géomagnétique le côté polaire du SETE devient plus abrupte. Celui-ci coïncide alors avec le bord polaire de la dépression de densité ionosphérique observée aux latitudes moyennes (MIT, mid-latitude ionospheric trough); il coïncide alors également avec le nouveau gradient de densité ionique formant la plasmapause à haute altitude.

La séquence des observations de COSMOS-900 montre clairement comment la dépression de densité ionosphérique aux moyennes latitudes se remplit, et comment le SETE est érodé pendant un orage géomagnétique. Ces résultats jettent un nouvel éclairage sur le mécanisme de formation de la plasmapause dans le secteur de temps local situé après 00:00 MLT, ainsi que sur la distribution du champ électrique dans cette même région avant et pendant un orage géomagnétique.

Samenvatting

De ionendichtheid N_i en de temperatuur van de electronen (T_e) opgemeten door de satelliet COSMOS-900 (gelanceerd op 30 maart 1977 in een polaire, circulaire baan : i= 83°, h = 500 km, periode = 94 min) worden gebruikt om het gedrag van de ionosfeer te bestuderen gedurende de magnetische storm van 1-2 december 1977. De ruimtelijke resolutie van de metingen bedraagt 0.3 breedtegraad voor T_e en ≤ 0.1 breedtegraad voor N_i. Er werden 27 omwentelingen opgetekend in het lokale geheugen van de satelliet. Dit laat een gedetailleerde analyse toe van de posities en breedte-profielen van de ionosfeer op gemiddelde breedten, en van de piek in de electronen temperatuur in de plaatselijke middernacht zone (SETE, Subauroral Electronic Temperature Enhancement). Gegevens omtrent de protonendichtheid die gelijktijdig werden gemeten door de satellieten "PROGNOZ-5" en "PROGNOZ-6" bevestigen dat de polaire rand van deze T_e-piek overeenkomt met de projectie van het magnetisch veld op de dichtheidsgradient die de plasmapause op grote hoogte vormt.

Gedurende de eigenlijke geomagnetische storm wordt polaire rand van de SETE zeer steil. Deze rand valt samen met een even steile polaire rand van de ionosfeer op gemiddelde breedtes, en met de nieuw gevormde gradient van de plasmapause op grote breedtes.

De verschillende observaties van COSMOS-900 tonen hoe de nachtzijde van de ionosfeer op gemiddelde breedtes zich opvult, en hoet de SETE en de buitenste lagen van de plasmasfeer eroderen gedurende een magnetische storm. Deze resultaten werpen een nieuw licht op de vorming van de plasmapause in de lokale tijdzone voorbij 00:00 MLT, en op het elektrisch veld in dezelfde regio tijdens een geomagnetische storm.

Zusammenfassung

Die Entwicklung der oberen Ionosphäre während des geomagnetischen Gewitters vom 1.-2. Dezember 1977 wurde mit Hilfe der vom am 30. Marz 1977 abgeschossenen Satelliten COSMOS-900 gemessenen Ionendichte N_i und Elektronentemperatur T_e untersucht. Die polare Umlaufbahn wies eine Neigung von i = 83° und eine Höhe h = 500 km sowie eine orbitale Zeit von 94 Minuten auf. Die Raumauflösung der Satellitenmessungen betrug ≤ 0.3 Grad Breite für Te und ≤ 0.1 Grad Breite für N1. Die Ergebnisse wurden an Bord in Grossraumspeichern registriert. Die sich über 27 aufeinanderfolgenden Umläufe erstreckenden Beobachtungen ermögenlichten die gründliche Ermittlung der Lage- und Verteilungsprofile von Dichte und Temperatur in dem nächtlichen Unterpolarlichtbereich, in dem eine Spitze der elektronischen Temperatur (SETE, Subauroral Electron Temperature Enhancement) festzustellen ist. Gleichzeitige Ermittlungen der Ionendichte in grossen Höhen mit dem PROGNOZ-5 und PROGNOZ-6 Satelliten bestätigen, dass der die Plasmapause bildende Dichtverlauf sich im Bereich des Polarrandes der SETE in die Ionosphäre projiziert.

Die Polarseite der SETE wird während der Hauptphase des geomagnetischen Gewitters steiler und entspricht dem Polarrand des Ionendichte-Abfalls bei mittleren Breiten (MIT, mid-latitude ionospheric trough) sowie dem neuen Ionendichte-Verlauf, der in grossen Höhen die Plasmapause bildet.

Die Reihenfolge der Beobachtungen von COSMOS-900 zeigen ganz klar, wie der Ionosphärendichte-Abfall in mittleren Breiten sich auffült und wie während eines geomagnetischen Gewitters die SETE abgetragen wird. Die Ergebnisse lassen die Bildung der Plasmapause im Zeitbereich nach Mitternacht sowie die Verteilung des elektrischen Feldes in demselben Bereich vor einem und während eines geomagnetischen Gewitters in neuem Licht erscheinen.

INTRODUCTION

More than two decades ago Muldrew (1965), Thomas and Andrews (1968), Rycroft and Thomas (1970), Rycroft and Burnell (1970), and Tulunay and Sayers (1971) have found mid-latitude ionospheric troughs (MIT) in the electron density N_e at F-region altitudes and above. They attempted to relate these MIT to the high altitude plasmapause as determined by Gringauz (1961) from the Soviet LUNIK observations and by early whistler measurements of Carpenter (1966) and others.

The correlation has been reasonably good on the nightside where the MIT is most clearly identified. Indeed, statistically the invariant latitude of this trough varies with Kp in a manner quite similar to the equatorial plasmapause density gradient. However, in the subsequent years, until 1986, this interpretation had been questioned since at times, and especially in the afternoon-dusk sector, the magnetic field lines corresponding to the high altitude plasmapause are located poleward of the ionospheric MIT in most cases when this feature could be identified (Grebowsky et al. 1976, 1978; Titheridge, 1976; Foster et al. 1978).

On the other hand using ISIS-1 observations Brace and Theis (1974) noted a distinct peak in the electron temperature (T_e) located within the steep N_e gradient of the middle latitude plasmapause on the nightside. They suggested that this subauroral electron temperature enhancement (SETE) corresponds to the field aligned projection of the high altitude plasmapause (PP), and that this temperature peak which is clearly identifiable at all local times down to at least 600 km altitude might be used to trace the movements of the plasmapause under variable geomagnetic conditions. However, they noted that the MLT distribution of the SETE did not exhibit the bulge in the dusk sector that is characteristic of the equatorial plasmapause as measured by whistler propagation (Carpenter, 1970) and by in situ satellite measurements (Chappell et al., 1971; Taylor et al., 1970).

The mid-latitude peak in T_e was not a new feature. Brace and Reddy (1965) and Brace et al. (1967) reported it as a nighttime phenomenon, already observed a decade earlier with an electrostatic probe onboard of EXPLORER-22 at an altitude of 1000 km. Other independent thermospheric electron temperatures measurements by a Langmuir probe on the polar-orbiting satellite ESRO-1, made before, during and after a geomagnetic storm, between October 31 and November 1, 1968, clearly confirmed the existence of a peak in ~~the~~ latitudinal electron temperature profiles in the subauroral region. This mid-latitude peak was observed at conjugated points in both hemispheres, in the altitude range 280-1500 km, and has been associated by Raitt (1974) with stable auroral red arcs (SAR arcs) observed in the midnight local time sector. The position of this electron temperature peak shifted to lower invariant latitude when K_p increased during the main phase of the geomagnetic storm. It moved slowly back to higher latitude during the recovery phase when K_p decreased. This equatorward and poleward shift of the SETE temperature peak was found to be very similar to the inward and outward motion of the equatorial plasmapause position, as observed by whistlers, and the position of SAR arcs. Similar results were reported by Brace et al. (1974) based on ISIS-2 polar satellite measurements (at 1400 km altitude). They traced the latitudinal shifts of the mid-latitude electron and ion temperatures peaks during the magnetic storm of August 4-6, 1972, with a time resolution of 2 hours UT, corresponding to the orbital period of ISIS-2. The occurrence frequency of well identified SETEs versus altitude was studied by Büchner et al. (1983) based on observations of INTERCOSMOS-18. They found that the occurrence frequency between 400 km and 800 km depends more strongly on altitude in the dayside local time sector than in the nightside one.

Although these low altitude observations tended to indicate an association between the SAR arcs, the mid-latitude electron temperature peak, and the mid-latitude ionospheric trough, the question remained as to how the subauroral electron temperature peak observed on average at an invariant latitude of 60° (L ~ 4) was really related to the location of the equatorial plasmapause. The answer to this question came more than a decade later from coordinated measurements of DE-2 and DE-1 satellites launched in August 1981. DE-1 traversed the plasmapause at altitudes of the order of 10,000 km, while DE-2 crossed the plasmapause L-shells at altitudes below 1000 km. Green et al. (1986) and Horwitz et al. (1986) found that the subauroral electron temperature enhancement in the 1900-2000 LT sector, occurs on field lines which thread the equatorward edge of a steep density gradient which is located inside the plasmasphere, closer to the Earth than the "whistler knee", at least in this MLT sector. To distinguish both steep plasma density gradients the former has been called the "inner plasmapause" while the latter is called the "outer plasmapause". The inner plasmapause has an almost circular magnetic local time MLT distribution unlike the outer plasmapause which may have a bulge in the afternoon-dusk sector. Brace et al. (1988) showed that this sharp internal gradient in plasmaspheric H^+ density marks the field lines of the F-region T_e ledge, i.e. that both features are physically associated and statistically lie on the same L-shells, near L=4 at magnetically quiet times.

Therefore, most of the contradicting results were based on observations in the afternoon-local time where it is now recognized that there are multiple plasmapause knees in the equatorial density profiles (see Carpenter et al., 1993). At night when, according to the classification of Horwitz et al. (1986), featureless plasmapause are observed most of the time, the correspondance between the MIT and equatorial plasmapause is most obvious.

In this paper we first examine simultaneous high time resolution measurements from the low altitude COSMOS-900 satellite on polar orbit, and, from the high altitude PROGNOZ-5 & 6 satellites, to confirm the close association between the SETE (subauroral electron temperature enhancement) and the high altitude PP (Plasmapause). In the second part of this study we describe how the profile and location of the SETE changes in the post-midnight sector during a large geomagnetic storm event. Due to their high time resolution these COSMOS-900 observations shade new light on the sequence of events during the erosion of the night side plasmasphere. They unravel also earlier views on the penetration of magnetospheric convection electric fields in the nightside plasmasphere.

2. PART 1 : THE PHYSICAL ASSOCIATION BETWEEN MID-LATITUDE IONOSPHERIC TROUGH (MIT), SUBAURORAL ELECTRON TEMPERATURE ENHANCEMENT (SETE) AND THE PLASMAPAUSE (PP) ION DENSITY GRADIENT

2.1. Description of the observations and spacecraft orbits

COSMOS-900 was launched on March 30, 1977 on a near-polar orbit with inclination of 83°, altitude of 500 km and orbital period of 1.5 hours. It operated for more than 2.5 years. During this time span PROGNOZ-5 and PROGNOZ-6 were operating on high altitude orbits with inclination of 65° and apogees of about 200,000 km altitudes. PROGNOZ-5 and 6 made plasma measurements at high altitudes over a wide range of invariant latitudes up to ± 65° (L ~ 5.6), like those of DE-1 which was launched four years later.

COSMOS-900 provided plasma observations in 1977 in the topside ionosphere, along an orbit similar to that of the DE-2 satellite, which was launched in 1981. The instrumentation on board of COSMOS-900 was designed to measure the electron temperature (T_e) and the ion density (N_i). The temperature T_e was measured by the method of r.f. (radio frequency) electron temperature probe, which is known as "rectification probe" and described in Afonin et al. (1973). This method was originally proposed by Aono et al. (1961). N_i was determined both by planar and spherical retarding potential analysers (RPA). The time resolution of T_e measurements was quite high : 4 seconds. The spherical RPA operated in "floating mode" of the outer grid, so that the time resolution for N_i measurements was equal to the telemetry rate : i.e. 1 second in the 1-day storage memory mode. Hence the spatial resolution was better than 0.3° and 0.1° in latitude respectively for T_e and N_i (i.e. 36 km and 12 km respectively). Thus these high time resolution data are suitable to study ionospheric features such as the mid-latitude ionospheric trough (MIT) and the subauroral electron temperature enhancement (SETE).

Note that the time resolution and consequently the spatial resolution of COSMOS-900 electron temperature measurements was more than a factor 3 higher than those of the ESRO-1 measurements of 1968 reported by Raitt (1974), and 30 times better than the ISIS-1 & 2 electron temperature observations of 1972 reported in Brace and Theis (1974) and Brace et al. (1974). The electron temperature measurements of 1981 made by DE-2 (Brace et al, 1988) had a spatial resolution of 40 km which was comparable to those COSMOS-900 (36 km). Therefore, COSMOS-900 enabled to resolve for the first time, in 1977, the extremely steep temperature gradient sometimes observed at the poleward edge of SETEs.

The RPA on board of PRGONOZ-5 and 6 are described in Gringauz et al. (1981) and Gringauz (1983). The high altitude measurements of the ion density (N_i) and ion temperature (T_i) have been obtained with a time resolution of 80 seconds.

2.2. Quiet time observations

During the periods of time considered below, the high and low altitude satellites traversed the plasmapause and MIT/SETE regions in the same local time sector. Fig. 1 shows the relevant parts of the orbits of COSMOS-900 and PROGNOZ-5 in L, MLT coordinates on 13 April 1977 which was a quiet day with K_p values of 2+, 0+, 2-, 1, 1+, 1+, 1, 2.

It can be seen that the orbits segments of both spacecraft are close to each other in the 2200-2400 MLT sector. COSMOS-900 traversed the magnetic shell L = 4 at 2:57 UT and again 1.5 hours later at 4:30 UT at an altitude of 510 km. The crossings off this magnetic shell by COSMOS-900 occurs almost 2 hours in local time later than that of PROGNOZ-5.

The ion densities (N_i) and electron temperatures (T_e) measured during these two consecutive traversals of the MIT are shown in fig. 2 as a function of L along COSMOS-900 orbits 217 (solid lines) and 218 (dashed lines) respectively. These measurements were made during quiet conditions (: K_p = O+) along COSMOS-900 orbits 217 and 218.

The PROGNOZ-5 ion density (N_i) and ion temperature (T_i) also shown in fig. 2 are measured at high altitudes between 8200 km and 14000 km. The altitudes of PROGNOZ-5 are given by the lower scale; the corresponding L is also given. PROGNOZ-5 traversed the magnetic shell L = 4 at 3:54 UT : i.e. 1 hour after COSMOS-900 did traverse this shell during orbit 217, and almost a half an hour before it did so again during orbit 218.

It can be seen that under these quiet conditions the subauroral electron temperature enhancements (SETE) have nearly symmetrical slopes on both sides of the T_e peak. Note also that the SETE is consistently located at the outer edge of the ion density gradient forming the equatorward boundary of the MIT. These results agree with those obtained by Brace and Theis (1974) using ISIS-1 Langmuir probe measurements at altitudes between 600 and 3000 km.

From the dotted line (N_i) in fig. 2 it can also be seen that the steep ion density gradient observed above 10,000 km altitude by PROGNOZ-5 is located at L = 4.8 : i.e. precisely between the L-shells where the SETE was observed by COSMOS-900, respectively one hour earlier (L = 4.3), and, a half an hour later (L = 5). This is consistent with an outward motion of the nightside plasmapause at a rate of 0.5 R_E/h, and, a simultaneous poleward motion of the SETE under quiet conditions or when K_p is decreasing. This outward motions of the nightside plasmapause during quiet conditions is supporting the existence of a continous, slow expansion of the plasmasphere (Lemaire and Schunk, 1994).

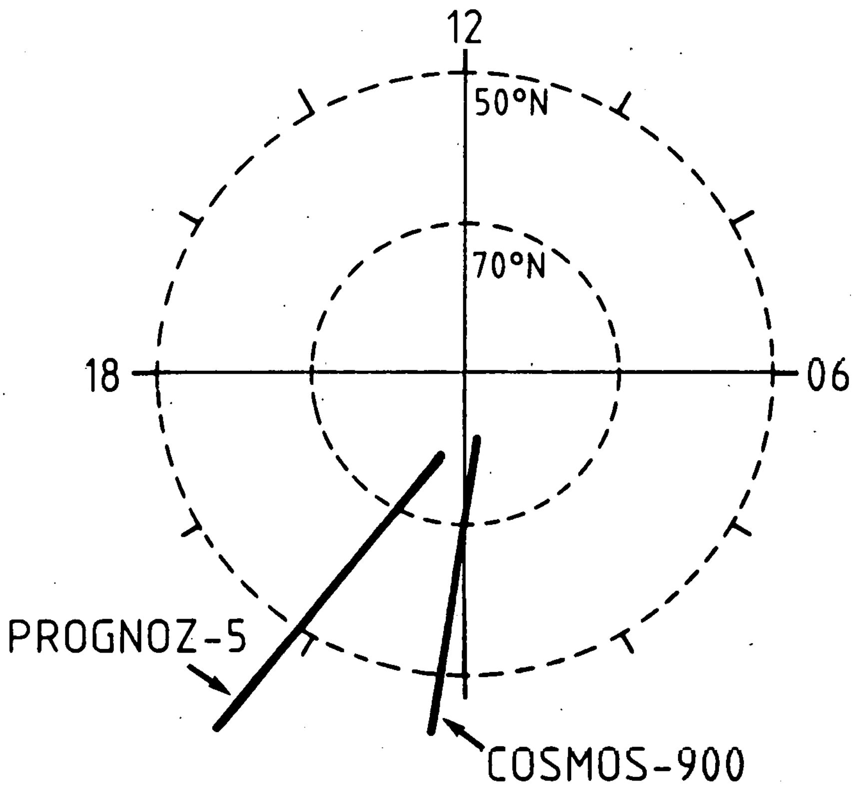

Fig. 1.-Projections of three orbits of COSMOS-900 on a MLT versus invariant latitude map in the northern hemisphere.

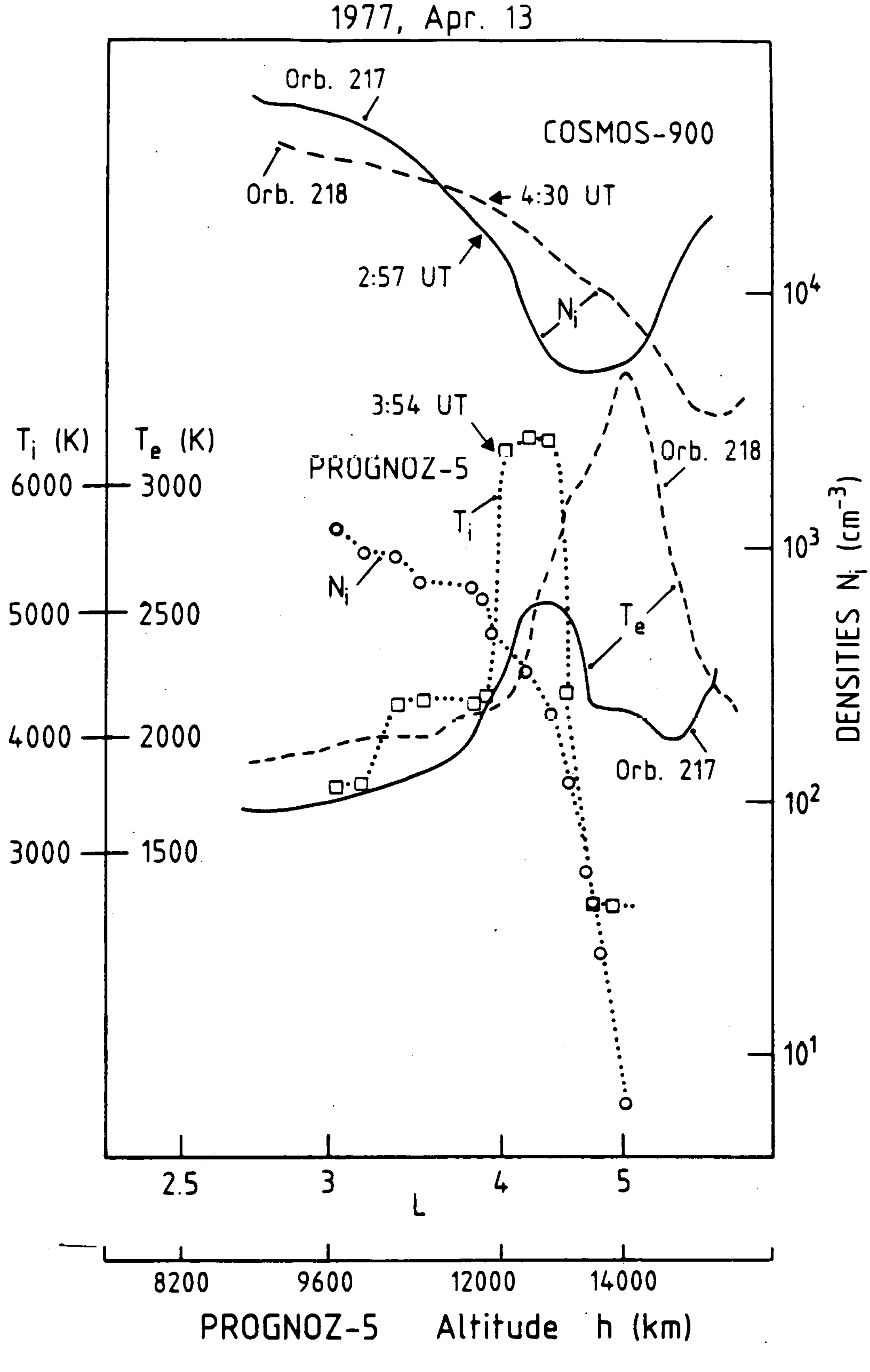

Fig. 2.-Low altitude ion densities (N_i) and electron temperatures (T_e) observed 13 April 1977, along two consecutive orbits of COSMOS-900 as a function of L. The dotted lines with open symbols give the ion density (N_i) and ion temperature (T_i) measured almost simultaneously at high altitude in the same MLT sector along PROGNOZ-5 orbit. The altitude of PROGNOZ-5 is shown on the scale at the bottom of the figure. These data correspond to quiet geomagnetic conditions.

PROGNOZ-5 was located in a local time sector more than one hour MLT closer to the duskside region than COSMOS-900. Therefore, one may argue that the universal time variations of the three plasmapause crossings is biaised by a possible local time variation of the position of the plasmapause. However, this is not likely to be the case according to the observations of Carpenter and Anderson (1992). Indeed, their ISEE measurements indicate that the equatorial plasmapause is closely circular in this LT sector, at least in a statistical sense.

The correspondence between the positions of SETE and of the high altitude plasmapause is consistent with DE-1/DE-2 observations indicating that both features are indeed related to each other and physically connected (Green et al., 1986; Kozyra et al., 1986, 1987; Brace et al., 1988). Horwitz et al. (1986) found evidence in the DE-2 measurements that the T_e enhancement in the F-region occurs on field lines which map into the plasmasphere or plasmapause region at a point where the density is about 10^3 cm^{-3}.

The dotted lines (T_i) in fig. 2 gives the ion temperature measured by PROGNOZ-5 at high altitude. It can be seen that the value of T_i increases in the outer region of the plasmasphere which has been called the "hot zone" by Gringauz and Bezrukikh (1976).

This enhancement of the high altitude ion temperature in the vicinity of the plasmapause is generally attributed to wave particle interactions. There are many papers dealing with this suggestion. But other plasma kinetic effects have also been proposed, e.g. the velocity filtration effect leading to positive ion temperature gradients in the outermost layer of the plasmasphere when the velocity distribution functions of the ions have an enhanced non-maxwellian tail (Pierrard and Lemaire, 1996). It is not the scope of this paper to discuss these heating mechanisms of the outer plasmasphere.

Since the peak of the high altitude ion temperature is located at a different (lower) L than the peaks of the low altitude SETE, we are tempted to conclude that both features are not on the same set of magnetic field lines, and, therefore are not directly related to each other : i.e. that the SETE is not a direct consequence of field aligned heat transferred from the high altitude hot ions to the ionospheric electrons.

As already indicated above we donot consider that the one hour difference in MLT of the COSMOS 900 and PROGNOZ-5 is likely to explain such an offset in the L-values of both temperature peaks.

2.3 Simultaneous observations at high and low altitudes during disturbed conditions

In the previous section we discussed simultaneous high and low altitude data obtained during quieting geomagnetic conditions. Fig. 3 illustrates observations obtained during disturbed conditions on 2 Dec. 1977 (see the K_p and D_{st} indexes for this period of time in fig. 5a).

The high altitude measurements of N_i were collected between 02:40 UT and 03:24 UT with PROGNOZ-6 in the altitude range 3700-8400 km in the 23 MLT sector, and for L ranging between 1.7 and 4.2. The high altitude plasmapause density gradient is observed at L = 3.1.

Corresponding COSMOS-900 data (T_e and N_i) were collected at lower altitude (480 km) in the 5-6 MLT sector. The solid and dashed lines in fig. 3 show the density and temperature profiles obtained respectively along two consecutive orbits (3771 and 3772) of COSMOS-900 when it moved from high latitudes to low latitudes across the MIT. The SETE was traversed at L = 3.2 (01:56 UT) and at L = 2.9 (03:31 UT). The MLT and invariant latitudes of the relevant portion of COSMOS-900 orbits 3764 to 3773 are shown in fig. 4.

Note that the T_e peaks have a much steeper poleward edges than in fig. 2. One might again consider that this is due to the variation of steepness of the electron temperature profile with local time, since the COSMOS-900 measurements shown in fig. 2 were obtained near midnight MLT, while those of fig. 3 refer to the dawn local time sector. But in the light of Carpenter and Anderson (1992), observations indicating that the steepness of the equatorial plasmapause is an increasing function of MLT, such an explanation does not hold. The most likely explanation is therefore that the midnight temperature profiles of fig. 2 were obtained during much quieter geomagnetic conditions than the steeper ones observed near dawn and shown in fig. 3. These conclusions are confirmed by the results shown below in fig. 6.

It is the sharp poleward edge of the SETE that has been used by Brace et al. (1988) in their statistical analysis of DE-2, to identify the location of the "inner plasmapause projection" at ionospheric heights. This characteristic signature of SETE can be identified in COSMOS-900 and DE-2 observations with an accuracy of a few tenths of a degree in latitude. Note that the maximum of T_e is usually located at a lower L value than this sharp poleward edge of the SETE. Note also that the slope of the equatorward wing of the SETE is not significantly steeper during disturbed conditions than it was during quiet times, as shown in fig. 2. Of course, this is not the case, for its poleward wing. The extreme sharpness of the poleward edge could not be resolved by the earlier Explorer-22, ISIS-1 & 2 and ESRO-1 probes, because of their lower time/spatial resolutions.

The steep plasmapause density gradient in the high altitude ion density was observed at 2:50 UT when PROGNOZ-6 traversed the shell L = 3.1. The near simultaneity in UT as well as the near coincidence in L of the plasmapause and SETE again confirm that there is a close physical relation between both features, even during disturbed geomagnetic conditions. This conclusion is based on the assumption that the shape of the plasmapause is nearly circular (i.e. independent on MLT) in the post-midnight sector. According to Carpenter and Anderson's (1992) statistical study of the plasmapause positions, this is a reasonable assumption.

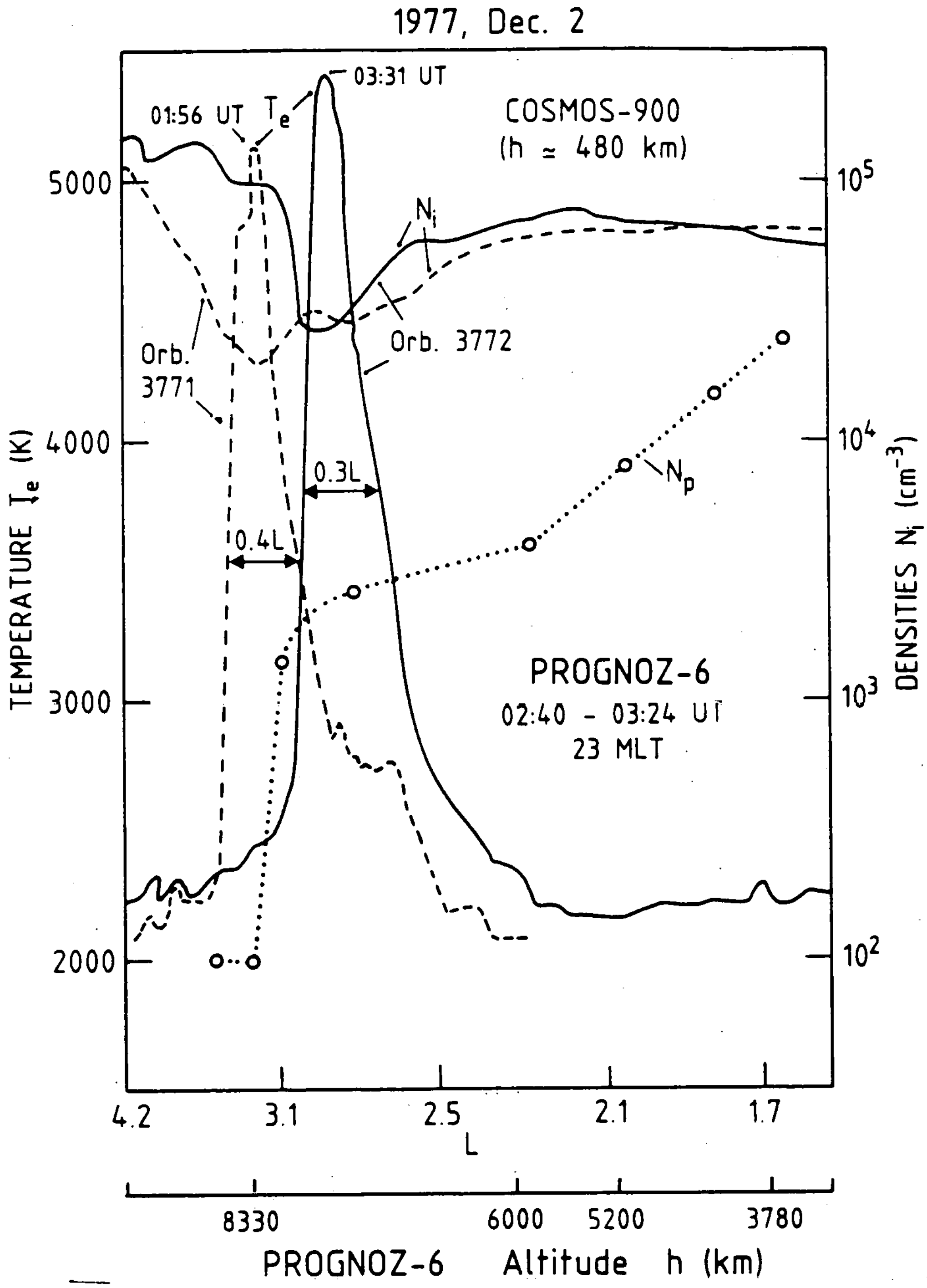

Fig. 3.-Low altitude ion densities (N_i) and electron temperatures (T_e) observed 2 December 1977, along two consecutive orbits of COSMOS-900 as a function of L. The dotted line with open circles gives the ion density (N_p) measured almost simultaneously in the same MLT sector along PROGNOZ-6 orbit at high altitude (see altitude scale at the bottom of the figure). These data sets are obtained during a period of increasing geomagnetic activity. Note the equatorward shift of the subauroral electron temperature enhancement when K_p increases.

Between orbits 3771 and 3772, K_p has increased from 5 to 7-. As a consequence of this enhanced geomagnetic activity, the nightside plasmapause is expected to form at smaller L, i.e. closer to Earth (Chappell et al., 1970), and the SETE is therefore expected to shift closer to the equator, as shown in fig. 3.

The magnitude of the electron temperature peak increases with increasing values of the magnetic activity index D_{st}. This was already mentionned by Büchner et al. (1983) and by Kozyra et al. (1986). It can be verified from fig. 3 that the width of the SETE at half peak value shrinked from 0.4L to 0.3L, during its equatorward shift, between the two consecutive orbits of COSMOS-900. This observation confirms again that the width of the SETE (at half peak height) is more narrow during disturbed conditions than during very quiet times. The reduction of this width is also consistent with the decrease of thickness of the equatorial plasmapause region when K_p increases (Chappell et al., 1970).

Having set the stage by describing in this first part the format of the COSMOS-900 observations and having also confirmed with independent data sets that the SETE is a reliable low altitude signature of the nightside equatorial plasmapause, we will now describe in detail the evolution of the position and shape of the SETE during the development of a geomagnetic storm. A number of statistical studies of the SETE locations and maximum peak temperatures have been published (see references already quoted above), but so far event *studies of the SETE during a geomagnetic storm* have not yet been published with spatial and time resolutions as high as those of COSMOS-900. The second part of this article aims to fill in this gap.

3. PART 2 : THE EVOLUTION OF THE SUBAURORAL ELECTRON TEMPERATURE ENHANCEMENT DURING A GEOMAGNETIC STORM

The data (N_i and T_e) presented below were collected along a set of consecutive orbits of COSMOS-900 (from orbit 3748 to 3776) including the period of the geomagnetic storm of 1-2 Dec. 1977. The invariant latitudes and magnetic local times along three of these orbits are shown in fig. 4. The data displayed in fig. 6 are all collected in the post-midnight local time sector. Fig. 5a shows the values of the K_p and D_{st} magnetic indexes during the time of observation. Before the geomagnetic storm started, K_p has been smaller than 2- for more than 12 consecutive hours.

At 15 UT December 1, COSMOS-900 is on its orbit 3764. The ion density (N_i) and electron temperature (T_e) measured during this orbit, under quiet (pre-storm) conditions, are shown as reference profiles on all 8 panels of fig. 6, by light solid lines. On the following orbit (3765) geomagnetic conditions are still quiet. This profile will correspond here to time t = 0: i.e. the beginning of the geomagnetic storm.

The density and temperature profiles shown by heavy solid lines in fig. 6a are almost the same as during the preceeding reference orbit (3764). The equatorward wing of the density trough did not change and has an exponentially decreasing slope. The subauroral electron temperature enhancement extends over 10° invariant latitude with a

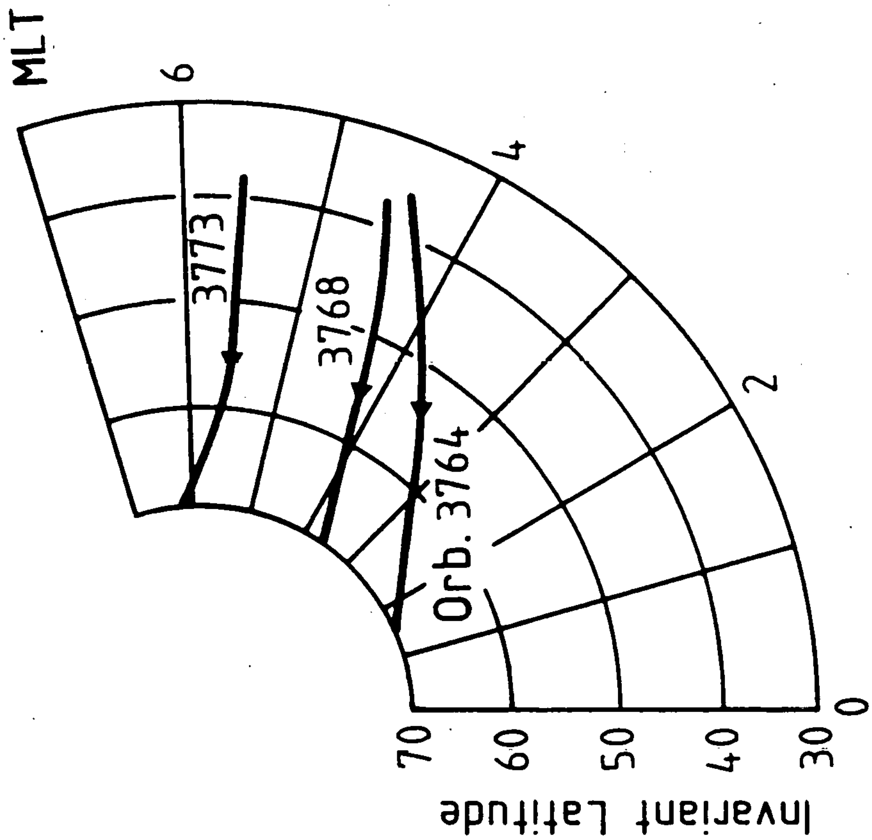

Fig. 4.-Projection three orbits of COSMOS-900 in the MLT versus invariant latitude map.

Fig. 5.-

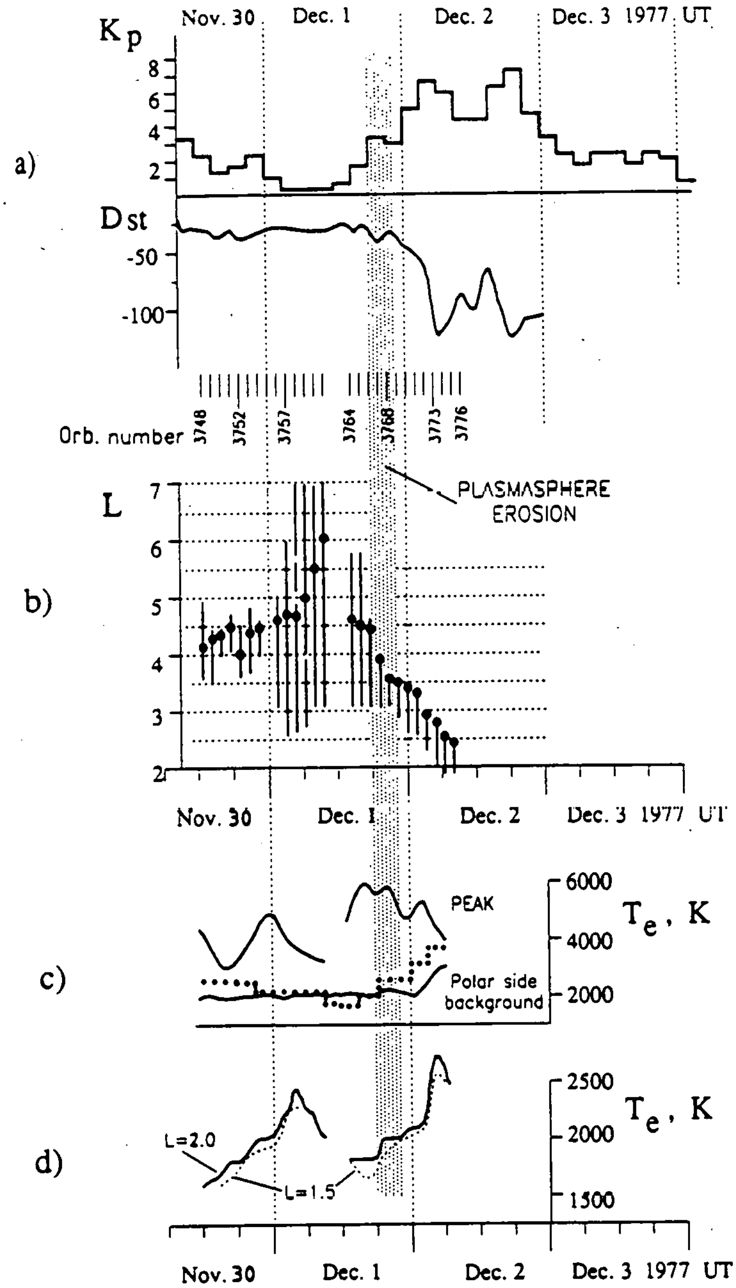

Fig. 5.-(Panel a) Values of the geomagnetic indexes K_p and D_{st} for a series of days in Nov. and Dec. 1977 including a large geomagnetic storm. The times corresponding to the relevant portions of orbits of COSMOS-900 are given by the orbit numbers from 3748 to 3776.

(Panel b) Values of L corresponding to the peak electron temperature (T_e) (solid dots) and width at half of the peak height (vertical bars) of the SETE as measured by along successive orbits of COSMOS-900 at low altitude (480 km) in the northern hemisphere in the post-midnight MLT sector.

(Panel c) Values of the peak electron temperature measured in the SETE by COSMOS-900. The temperature in the auroral region poleward of the mid-latitude ionospheric trough is also shown.

(Panel d) Values of the effective temperature of the electrons at L = 2 (solid line)and L = 1.5 (dashed line) on the equatorward side of the SETE. These effective temperature measurements are obtained from the determination of the slope of current-voltage characteristics over an interval centered around the floating potential of the spacecraft.

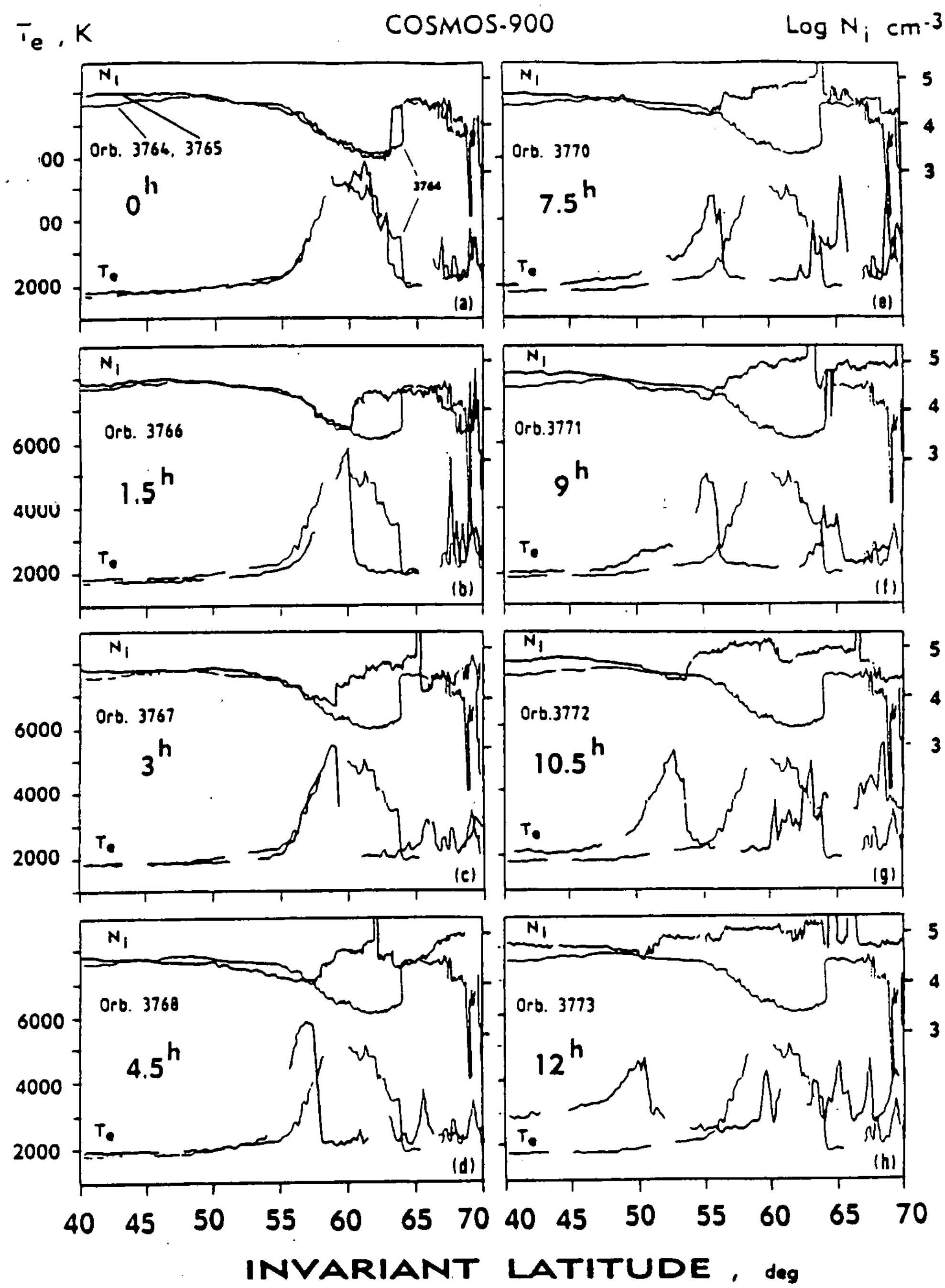

Fig. 6.- Illustration of the evolution of the ion density (N_i) and electron temperature (T_e) profiles versus L, before and during the main phase of the geomagnetic storm of Dec. 1-2, 1977. The high spatial resolution (12 km)of the ion measurements and (36 km) of the electron temperature measurements enabled to determine (for the first time in 1977) the extreme steepness of these density and temperature profiles. The equatorward shift of the auroral ionization is shown. The associated erosion of the poleward wing of the SETE (and of the corresponding high altitude plasmasphere) are also evidenced in this unique series of observations. The orbital period of COSMOS-900 is 1.5 h. This governs the time recurrence of each set of observations. In each of the 8 panels the density and temperature profiles corresponding to the prestorm orbit (n° 3764) have been given for comparison. Note that it take 3-4 hours after the beginning of the geomagnetic storm before the ionization front and the steepened poleward ledge of the SETE has moved to invariant latitudes lower than that of the peak temperature of the prestorm SETE.

maximum T_e value of 5000-6000 K at 58-62°. Small scale structures are present on the poleward side of the temperature peak.

It can also be seen that the poleward side of the ion density trough has an extremely steep gradient forming a "wall" or ledge on the equatorward side of the auroral region. In the time period of 1.5 hours, between orbit 3764 and 3765, this "wall" has shifted equatorward from 64° to 63° invariant latitude. This shift is a result of the slight increase of geomagnetic activity : indeed, K_p has increased from 1- to 2- during that period of time (see fig. 5a).

An additional increase of K_p to a value of 3+ occured during the following orbits (3766 & 3767) of COSMOS-900, respectively at t = 1.5 h & 3 h. The result is an additional shift of the sharp auroral density "wall" down to 60° invariant latitude as can be seen in fig. 6b and 6c. It can also be seen in these panels that the poleward wing of the subauroral electron temperature enhancement has changed from a rather irregular slope of about 1000 K/degree latitude to a steep negative gradient larger than 40,000 K/degree latitude. This ledge in the temperature profile is precisely located at the same latitude as the positive density "wall": the ledge of the SETE moves equatorward with the same speed as the auroral density "wall". However, so far the equatorward wing of the temperature enhancement remains unchanged during this initial period of time. Only the poleward wing of the SETE is modified due to the equatorward propagation of the auroral ionization density front.

The trend outlined above continues during the following orbits of COSMOS-900 for 12 hours since (i.e. until orbit 3773 shown in fig. 6h), while K_p increased progressively up to a maximum value of 7- on 2 Dec. 1977 between 03 and 06 UT. By that time, D_{st} has reached, its minimum value and the density "wall" has reached an invariant latitude as low as 51° (L ≅ 2.52). But, note that it is only 3 or 4 hours after the beginning of the storm, that the wing of the temperature profile equatorward of the peak starts moving southward (see fig. 6d corresponding to orbit 3768 at t = 4.5 h). It is important to emphasize that during the 3 or 4 first hours the invariant latitude of the temperature peak did not change. The temperature and density distributions on the equatorward wing of the SETE did not change either during these first 3 or 4 hours after the onset of the geomagnetic storm.

The existence of SETEs with extremely sharp poleward edges was also found in the observations of DE-2 which had a time resolution similar to those of COSMOS-900 (Brace et al. 1988). But, as emphasized above, during very quiet conditions, this sharp ledge is absent and becomes a rather irregular temperature profile as shown in fig. 6a. The irregular small scale structures of T_e are attributed to irregular magnetospheric particle precipitation patterns.

The solid dots in fig. 5b indicate the positions (L) of the subauroral electron temperature enhancement, well before the geomagnetic storm commencement (orbit 3748), up to orbit 3776, after the main phase. The vertical line segments correspond to the latitudinal extent of the SETE. During Nov. 30, and early Dec. 1, the position of the equatorial plasmapause (as identified by the SETE in the ionosphere) moves to higher L, while K_p decreased during this period of time. This is in agreement with the relationship

$$L_{pp} = 5.6 - 0.46\, K_{pmax} \qquad (1)$$

where K_{pmax} is the maximum K_p value in the preceding 24 hours. This relation was first proposed by Carpenter and Park (1973) and recently confirmed by Carpenter and Anderson (1992).

From their statistical study based on DE-2 observations, Brace et al. (1988) found similar relationships depending on the value of K_p' which is a modified K_p index defined as following : K_p' is the highest 3-hour K_p value which occured during the 12-hour period preceding the measurements. This magnetic parameter was also adopted by Kozyra et al. (1986) because it provided the best ordering of the T_e signatures. The use of K_{pmax} or K_p' rather than the 3-hour K_p recognizes that the expansion of the plasmapause following substorm activity is slow because the refilling process has a time constant of several days.

Brace et al. (1988) found that the locations of the T_e maximum at nightside fit the linear relation

$$L' = 6.06 - 0.6\, K_p' \qquad (2)$$

This relation was deduced from DE-2 data during solar maximum conditions (i.e. in 1981). From AE-C measurements during solar minimum (1976-77), Brace (1990) finds a different relation for the nightside SETE location

$$L'' = 5.40 - 0.34\, K_p' \qquad (3)$$

Fig. 7 shows the values of L', L" and Lpp predicted by eqs. (1), (2) and (3). These predictions are compared to the T_e peak positions (dots) observed by COSMOS-900 which were obtained during solar minimum conditions. It can be seen that the relationship of Brace et al. (1988) approximately fits the COSMOS-900 observations. But, as already shown in fig. 6, it is only 3 h. after the storm commencement that the position of the T_e maximum begins to shift to more innerward magnetic shells. This time lag of 3 h. can hardly be appreciated in fig. 7 since the time resolution of K_{pmax} and K_p' indexes is equal to 3 h. However, this time lag is clearly evident in fig. 6.

In other words, the location of plasmapause as derived from the position of the SETE in the post-midnight sector does not shift to lower L-values immediately after the onset of a geomagnetic storm or substorm. It takes a certain lapse of time (3-4 h) before the erosion or peeling of the nightside plasmasphere takes place at lower magnetic shells. This delay corresponds to the time which is needed for the auroral ionization front to drift from high invariant latitudes (> 65°) across the mid-latitude ionospheric trough.

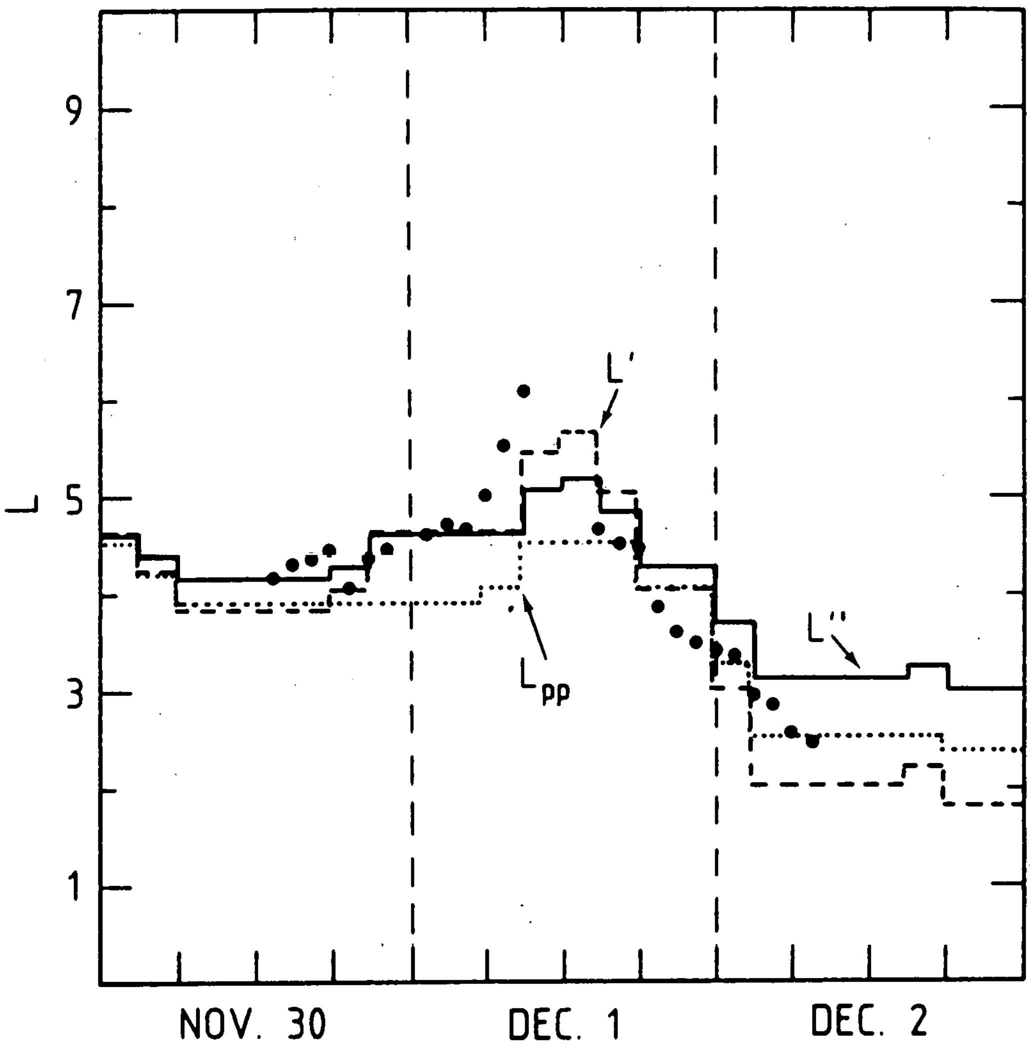

Fig. 7.- Values of L', the location of the SETE peak temperature in the nightside versus universal time as predicted by the relation (2) determined by Brace et al. (1988) from DE-2 Langmuir probe electron temperature measurements ($T_{e,cold}$) for solar maximum conditions. The modified K_p' index giving the highest K_p-value during the 12-hour period preceding the measurements, has been used to determined L' and L" given by eq (3) for solar minimum conditions from AE-C observations. The equatorial plasmapause positions (L_{pp}) predicted by eq. (1) determined by Carpenter and Park (1973) from whistler observations is also shown for the period corresponding to the Dec. 1-2 geomagnetic storm. The solid dots give the L-values corresponding to the SETE peak temperature as measured by COSMOS-900 during this period of time.

F-region signatures, including zonal ion velocities associated with dc electric fields in a different (dusk) sector have shown a similar time delay of 3-6 hours for a geoelectric disturbance to propagate from high latitude to lower latitudes (Miller et al., 1990).

4. INTERPRETATION OF THE RESULTS AND DISCUSSION

1. Non-uniform enhancement of the electric field. Our results indicate that the erosion of the plasmasphere takes place in the post-midnight local time sector, when and where the equatorward edge of the auroral region is shifting closer to the equator and reaching magnetic field lines corresponding to the location of the quiet time SETE maximum. At high altitude in the magnetosphere this should be associated with the sunward motion of a cloud of plasmasheet particles. If this interpretation is correct, the convection electric field within this plasma cloud must have an enhanced westward component. The existence of a westward E-field is supported by the observed equatorward shift of the auroral ionization front shown in fig. 6.

Equatorward to this propagating ionization front the latitudinal distribution of the ionospheric plasma density is unperturbed during the first 3 or 4 hours following the beginning of the geomagnetic strom in the early phase of the storm. This implies that the convection velocity is unchanged there. This implies also that the convection electric field (as measured in a frame of reference corotating with the Earth) has a nearly zero westward component on the equatorward side of the propagating ionization "wall", while this westward E-field component is non-zero on its poleward side. In other words, during the inital phase of a magnetic storm, the convection electric field distribution may correspond to that of a finger-like plasma cloud intruding into an almost unperturbed plasmatrough and eventually into the nightside plasmasphere. This tentative interpretation needs to be checked with future global imaging missions to the magnetosphere.

At a fixed instant of time, the westward electric field component is not enhanced at all magnetic shells, contrary to what is currently assumed in K_p-dependent convection electric field models, like for instance the shielded Volland-Stern models (Volland, 1973, 1975, 1978; Stern, 1977). Indeed, in these electric field models the dawn-dusk component of the E-field is assumed to change in phase with K_p simultaneously at all locations in the magnetosphere. The results illustrated in fig. 6 indicate that this was not the case on Dec. 1, 1977: the time-dependent convection electric field associated with the magnetic storm was not an uniformly distributed enhancement of the dawn-dusk component. The effects of the inward propagating electric field enhancement were observed first on the more distant magnetic shells, and only later on those closer to Earth.

More general and structured dynamical electric field models of the magnetosphere taking into account this effect are required in the future to interpret high resolution observations like illustrated in fig. 6 (see also Carpenter, 1995).

Indeed, important effects have been ignored in earlier quasi-static and time-dependent magnetospheric convection electric fields e.g. 1) large induced electric fields which, recently, have been shown to be of paramount importance during geomagnetic storm (Li et al. 1993, 1994; Hudson et al. 1995); 2) finite gyroradius effects resulting from the different mass and momentum of electrons and ions (Lemaire et al., unpublished manuscript, 1996). The latter effects are ignored in MHD models as well as in kinetic models based on the guiding center approximation. This leads to the general conclusion that space weather models of the magnetosphere cannot exclusively be build on a global/large scale magnetospheric convection flow pattern. As in meteorology, they will have to take into account the existence and the effects of sharp "fronts" separating cold and hot air masses or plasma volumes in the magnetosphere.

Present day magnetospheric convection models are unable to explain the observations reported in fig. 6 i.e. the sharpness of the plasma density "wall", the sharpness of the poleward edge of the SETE, and the time evolution of its erosion during the geomagnetic storm of Dec. 1, 1977.

2. Interface between hot and colder plasma clouds. The ionization "wall" at the equatorward edge of the auroral region is considered to be the projection of the inner edge of the plasmasheet. We propose that it corresponds to the field aligned projection of a sharp surface separating, on one side, hot plasma of the plasmasheet, and on the other side the colder plasma in the plasmatrough or plasmapause region. This interpretation is supported by a quantitative kinetic model recently developed by Lemaire et al. (1996).

3. Asymmetric erosion of SETE. The widths of the SETE wings on both sides of the T_e maximum are indicated by vertical lines in fig. 5b. It can be seen that during quiet geomagnetic conditions (pre-storm) the SETE extends in a symmetrical way on both sides.

Furthermore, during the first 3-4 hours corresponding to orbits 3765-66, fig. 5b indicates that the low latitude wing of the SETE remains unperturbed while the poleward wing is rapidly eroded. There is no additional heat deposition equatorward of the SETE maximum during this initial phase. It is only 3-4 hours after the storm commencement that this part of the mid-latitude ionosphere is gradually heated. The ionospheric temperature at Λ = 40-45° remains unchanged for almost ten hours. The first indication of a temperature increase is seen in fig. 6g (at t = 10.5 h).

Twelve hours after the storm commencement the maximum peak temperature has moved down to Λ = 51° (L = 2.5) but the width of the propagating temperature enhancement has remained approximately constant (see fig. 5b and fig. 6d-h).

4. Assocation between N_i and T_e ledges. The peaks in electron temperature are known to coincide with SAR arcs when the latter are observable. They are considered to be caused by plasmaspheric electron heated by Coulomb collisions with ring current protons (Cole, 1965) and O^+ ions (Kozyra et al., 1987). Cornwall et al. (1971) proposed

Landau damping of ions cyclotron waves as an alternate way of heating the cold plasmaspheric electrons (< 1 eV). These heating mechanisms take place in the plasmapause region where cold plasma is overlaping with the ring current region. In all cases the electron heat is conducted from the high altitude plasmapause region into the underlying F-region, where particles forming the tail of the electron velocity distribution excite the $O(^1D)$ state of neutral atomic oxygen. Later de-excitation of the oxygen atoms produces the emission at 630 nm that is observed as a red arc (SAR arc) observed from ground.

Kozyra et al. (1987) found also that rather symetric profiles of T_e associate with SAR arcs which are generally observed during the storm recovery phase, are consistent with the equatorial density profiles of ring current O^+ ions of energies of 10-20 keV. However, no explanation has yet been proposed for the steep temperature gradient formed during the initial and main phase of a magnetic storm on the poleward wing of SETE. By now all what the sequence of N_i and T_e profiles of fig. 6 are able to tell us, is that the sharp ionospheric temperature gradient is closely associated with the propagating auroral ionization "wall" during the main phase of the storm. This association between N_i and T_e ledges is not yet understood and needs more investigations. This issue is beyond the grasp of this paper and our observations, of course, are unable to resolve this question.

5. Variation of electron temperature peak with magnetic activity. The upper solid lines in fig. 5c show the value of the peak temperature measured by COSMOS-900 before and during the storm. These peak values vary between 3000 K and 6000 K. From DE-2 observations in the altitude range 350-600 km, Kozyra et al. (1986) found a linear variation of the nightside $T_{e,max}$ as a function of K_p' :

$$T_{e,max} = 1570 + 318\ K_p' \qquad (4)$$

The predictions of this linear fit are shown by the dotted line in fig. 5c. It can be seen that the maximum temperature values predicted by this relation (dotted line) are much lower than those measured by COSMOS-900 in 1977 (upper solid lines). This difference may be accounted for by the large scatter of DE-2 data around the statistical relation (4) (see fig. 8 in Kozyra et al., 1986), but it is more likely due to the different methods used to determine the electron temperature, respectively, from COSMOS-900 and DE-2 measurements.

Indeed, from the DE-2 Langmuir probe measurements a temperature, $T_{e,cold}$, for the cold maxwellian ionospheric electrons was deduced; indeed, these cold electrons contribute to most of the total flux measured by Langmuir probes. On the contrary, the electron temperature obtained from the COSMOS-900 measurements were determined by the slope of the current-voltage characteristics (I-V curves) averaged over an electric potential interval $\Delta V \cong kT_e/e$, which is centered around the floating potential of the probe. The electrons were assumed to have a maxwellian velocity distribution function. However, if the electrons have a non-maxwellian velocity distribution (e.g. Lorentzian velocity distribution) with a population of supra-thermal electron forming an extended tail, the values of the effective electron temperature ($T_{e,eff}$) deduced from the slope of the current-voltage characteristic are systematically larger than $T_{e,cold}$ obtained from Langmuir probe flux measurements.

Direct comparison of r.f. probe measurements and spherical Langmuir probe measurements of electron energy spectra have been compared by Afonin et al. (1975) using COSMOS-378 data between 240 km and 1750 km altitude. The presence of non-maxwellian electron velocity distributions may explain that the peak temperature values ($T_{e,eff}$) shown in fig. 5c are significantly higher than the values of $T_{e,cold}$ predicted by eq. (4) which was deduced from DE-2 Langmuir probe average electron temperature measurements.

Since the definitions of $T_{e,cold}$ and $T_{e,eff}$ are different for the reasons indicated above, they cannot be directly compared to each other, and their variation need not necessarily to follow the same trend during geomagnetic storms, as indeed shown in fig. 5c.

Kozyra et al (1986) deduced from their statistical study of SETE that the magnitude of the electron temperature peak $T_{e,max}$, increases with increasing value of the D_{st} magnetic activity index. For altitudes below 600 km on the nightside they found

$$T_{e,max} = 2513 - 8\,D_{st} \qquad (5)$$

Similar results were obtained by Büchner et al. (1983) from INTERCOSMOS-18 Langmuir-probe observations. The COSMOS-900 results shown in fig. 5c do not well support this statistical prediction (not shown). The lack of agreement may be due (i) to the large scatter of DE-2 (as shown in fig. 9 of Kozyra et al., 1986), and, (ii) to the different method used to determine the electron temperatures from DE-2 and COSMOS-900 data, respectively.

6. Electron temperature on the poleward side of the SETE. The ionospheric electron temperature on the polar side of the SETE is shown by the lower solid line of fig. 5c. This background temperature on the poleward side does not change during the storm, except after orbit 3770 (after 24.00 UT, on Dec. 1, 1977) i.e. well within the main phase of the geomagnetic storm. This implies that nearly no energy is transfered from the ring current particles except in the plasmapause region where the distribution of ring current particles overlaps with the cold plasmaspheric electrons.

7. Electron temperature on the equator side of the SETE. Fig. 5d shows the change of the electron temperature in the post-midnight sector at low latitudes : at L = 1.5 (dashed line) and at L = 2.0 (solid line). Note the reduced temperature scale compared to fig. 5c. It can be seen that the low latitude temperatures do not exceed 3000 K, even during the main phase of the geomagnetic storm.

ACKNOWLEDGEMENTS

One of the authors (J.F. Lemaire) thanks the Belgian Institute for Space Aeronomy and the Services Fédéraux des Affaires Scientifiques, Techniques et Culturelles, who are supporting the collaboration between IKI and IASB. It is in the framework of this collaboration that this paper has been prepared, based on data collected by Russian satellites more than 15 years ago. We thank the referees for useful comments.

REFERENCES

AFONIN, V.V., GDALEVICH, G.L., GRINGAUZ, K.I., KAINAROVA, Ja., SMILAUER, Ja., Ionospheric studies conducted by the satellite Intercosmos-2. III. Ionospheric electron temperature measurements by high-frequency probe method, Cosmic Research, V.11, 254-264, 1973.

AFONIN, V.V., GDALEVICH, G.L. and SHERONOVA, S.M., Ionospheric study with COSMOS-378 satellite, Geomagn. I. Aeronom., 15, N4, 615-620, 1975.

AONO, Y., HIRAO, K. and MIYAZAKI, S., Positive ion density, electron density and electron temperature by Kappa-8-5 and 6 rockets, J. Radio Res. Lab., 8, 453-465, 1961.

BRACE, L.H., Solar cycle variations in F-region T_e in the vicinity of the midlatitude trough based on AE-C measurements at solar maximum, Adv. Space Res., 10(11), 83-88, 1990.

BRACE, L.H., CHAPPELL, C.R., CHANDLER, M.O., COMFORT, R.H., HORWITZ, J.L. and HOEGY, W.R., F region electron temperature signatures of the plasmapause based on Dynamics Explorer 1 and 2 measurements, J. Geophys. Res., 93, 1896-1908, 1988.

BRACE, L.H., MAIER, E.J., HOFFMAN, J.H., WHITTEKER, J. and SHEPPERD, G.G., Deformation of the night side plasmasphere and ionosphere during the August 1972 geo-magnetic storm, J. Geophys. Res., 79, 5211-5218, 1974.

BRACE, L.H. and REDDY, B.M., Early electrostatic probe results from Explorer-22, J. Geophys. Res., 70, 5783-5792, 1965.

BRACE, L.H., REDDY, B.M. and MAYR, H.G., Global behavior of the ionosphere at 1000 kilometer altitude, J. Geophys. Res., 72, 265-283, 1967.

BRACE, L.H. and THEIS, R.F., The behavior of the plasmapause at mid-latitudes : ISIS 1 Langmuir probe measurements, J. Geophys. Res., 79, 1871-1884, 1974.

BRACE, L.H., CHAPPELL, C.R., CHANDLER, M.O., COMFORT, R.H., HORWITZ, J.L. and HOEGY, W.R., F region electron temperatutre signatures of the plasmapause based on dynamics Explorer 1 and 2 measurements, Jour. Geophys. Res., 93, A3, 1896-1908, 1988.

BÜCHNER, J., LEHMANN, H.R. and RENDTEL, J., Properties of subauroral electron temperature peak observed by Langmuir-probe measurements on board Intercosmos-18, Gerlands Beitr. Geophys., 92, 368-373, 1983.

CARPENTER, D.L., Whistler evidence of the dynamic behavior of the duskside bulge in the plasmasphere, J. Geophys. Res., 75, 3837-3847, 1970.

CARPENTER, D.L., Whistler studies of the plasmapause in the magnetosphere. 1. Temporal variations in the position of the knee and some evidence on plasma motions near the knee, J. Geophys. Res., 71, 693-709, 1966.

CARPENTER, D.L., Earth's plasmasphere awaits rediscovery, EOS, Trans. AGU, 76(9) p. 89-92, 1995.

CARPENTER, D.L. and ANDERSON, R.R., An ISEE/whistler model of equatorial electron density in the magnetosphere, J. Geophys. Res., 97, 1097-1108, 1992.

CARPENTER, D.L., GILES, B.L., CHAPPELL, C.R., DECREAU, P.M.E., ANDERSON, R.R., PERSOON, A.M., SMITH, A.J., CORCUFF, Y. and CANU,

P., Plasmasphere dynamics in the duskside bulge region; a new look at an old topic, J. Geophys. Res., 98, 19243-19271 1993.
CARPENTER, D.L. and PARK, C.G., On what ionosphere workers should know about the plasmapause-plasmasphere, Rev. Geophys. Space Phys., 11, 133-154, 1973.
CHAPPELL, C.R., HARRIS, K.K. and SHARP, G.W., A study of the influence of magnetic activity on the location of the plasmapause as measured by Ogo 5, J. Geophys. Res., 75, 50-56, 1970.
CHAPPELL, C.R., HARRIS, K.K. and SHARP, G.W., The dayside of the plasmasphere, J. Geophys. Res., 76, 7632-7647, 1971.
COLE, K.D., Stable auroral red arcs, sinks for energy of D_{st} main phase, J. Geophys. Res., 70, 1689-1706, 1965.
CORNWALL, J.M., CORONITI, F.V. and THORNE, R.M., Unified theory of SAR arc formation at the plasmapause, J. Geophys. Res., 76, 4428-4435, 1971.
FOSTER, J.C., PARK, C.G., BRACE, L., BURROWS, J.R., HOFFMAN, J.H., MAIER, E.J. and WHITTEKER, J.H., Plasmapause signatures in the ionosphere and magnetosphere, J. Geophys. Res., 83, 1175-1182, 1978.
GREBOWKSY, J., MAYNARD, N., TULUNAY, Y. and LANZEROTTI, L., Coincident observations of ionospheric troughs and the equatorial plasmapause, Planet. Space Sci., 24, 1177-1185, 1976.
GREEN, J.L., WAITE, J.H., Jr., CHAPPELL, C.R., CHANDLER, M.O., DOUPNIK, J.R., RICHARDS, P.G., HEELIS, R., SHAWHAN, S.D. and BRACE, L.H., Observations of ionospheric magnetospheric coupling : DE and Chatanika coincidences, J. Geophys. Res., 91, 5803-5815, 1986.
GRINGAUZ, K.I., The structure of the Earth's ionized gas envelope based on local charged particle concentrations measured in USSR, Space Research, II, 574-592, 1961.
GRINGAUZ, K.I., Plasmasphere and its interaction with the ring current, Space Science Reviews, 34, 245-257, 1983.
GRINGAUZ, K.I. and BEZRUKIKH, V.V., Asymmetry of the Earth's plasmasphere in the direction noon-midnight from PROGNOZ-1 and PROGNOZ-2 data, J. Atmos. Terr. Phys., 38, 1071-1076, 1976.
GRINGAUZ, K.I., BEZRUKIKH, V.V. and AFONIN, V.V., The plasmasphere physics problems in the light of the measurements from Prognoz-5, Book of abstracts, Turkmeniam Academy of Sci., All-Union Conference on the Results of IMS-Project, Ashabad, p. 17, 1981.
HORWITZ, J.L., BRACE, L.H., COMFORT, R.H. and CHAPPELL, C.R., Dual-spacecraft measurements of plasmasphere-ionosphere coupling, J. Geophys. Res., 91, 11203-11216, 1986.
HUDSON, M.K., KOTELNIKOV, A.D., LI, X., ROTH, I., TEMERIN, M., WYGANT, J., BLAKE, J.B., GUSSENHOVEN, M.S., Simulation of proton radiation belt formation during the March 24, 1991 SSC, Geopys. Res. Lett., 22, 291-294, 1995.
KOZYRA, J.U., BRACE, L.H., CRAVENS, T.E. and NAGY, A.F., A statistical study of the subauroral electron temperature enhancement using Dynamics Explorer 2 Langmuir probe observations, J. Geophys. Res., 91, 11270-11280, 1986.

KOZYRA, J.U., SHELLEY, E.G., COMFORT, R.H., BRACE, L.H., CRAVENS, T.E. and NAGY, A.F., The role of ring current O^+ in the formation of stable auroral red arcs, J. Geophys. Res., 92, 7487-7502, 1987.

LEMAIRE, J. and SCHUNK, R.W., Plasmaspheric convection with non-closed streamlines, J. Atm. Terr. Phys., 56, 1629-1633, 1994.

LEMAIRE, J.F., ROTH, M. and DEKEYSER, J., EMF driver of subauroral ion drifts, Aeronomica Acta A n° 399, (unpublished manuscript, 1996).

LI, X., ROTH, I., TEMERIN, M., WYGANT, J.R., HUDSON, M.K. and BLAKE, J.B., Simulation of the prompt energization and transport of radiation belt particules during the March 24, 1991 SSC, Geophys. Res. Lett., 20, 2423-2426, 1993.

LI, X., HUDSON, M.K., BLAKE, J.B., ROTH, I., TEMERIN, M. and WYGANT, J.R., Observation and simulation of the rapid formation of a new electron radiation belt during March 24, 1991 SSC, Proceedings of Workshop on Earth's Trapped Particle Environment, Aug. 14-19, 1994, Taos, (preprint, 1995).

MILLER, N.J., BRACE, L.H., SPENCER, N.W. and CARIGNAN, G.R., DE 2 observations of disturbances in the upper atmosphere during a geomagnetic storm, J. Geophys. Res., 95, 21.017-21.031, 1990.

MULDREW, D.B., F layer ionization troughs deduced from Alouette data, J. Geophys. Res., 70, 2635-2650, 1965.

PEYRIMAT, C. and FONTAINE, D., Numerical simulation of magnetospheric convection including the effect of field-aligned currents and electron precipitation, J. Geophys. Res., 90, 11.155-11.176, 1994.

PIERRARD, V. and LEMAIRE, J., Lorentzian model ion-exosphere (accepted in JGR) 1996.

RAITT, W.J., The temporal and spatial development of mid-latitude thermospheric electron temperature enhancements during a geomagnetic storm, J. Geophys. Res., 79, 4703-4708, 1974.

RYCROFT, M.J. and BURNELL, S.J., Statistical analysis of movements of the ionospheric trough and the plasmapause, J. Geophys. Res., 75, 5600-5604, 1970.

RYCROFT, M.J. and THOMAS, J.O., The magnetospheric plasmapause and the electron density trough at the Alouette-1 orbit, Planet. Space Sci., 18, 65-80, 1970.

STERN, D.P., Large-scale electric fields in the Earth's mangetosphere, Rev. of Geophys. and Space Physics, 15, 156-194, 1977.

TAYLOR, H.A., BRINTON, H.C. and DESHMUKH, A.R., Observations of irregular structure in thermal ion distributions in the duskside magnetosphere, J. Geophys. Res., 75, 2481-2489, 1970.

THOMAS, J.O. and ANDREWS, M.K., Transpolar exospheric plasma. 1. Plasmasphere termination, J. Geophys. Res., 73, 7407-7417, 1968.

TITHERIDGE, J.E., Plasmapause effects in the topside ionosphere, J. Geophys. Res., 81, 3227-3233, 1976.

TULUNAY, Y. and SAYERS, J., Characteristics of the mid-latitude trough as determined by the electron density experiment on ARIEL III, J. Atmos. & Terr. Phys., 33, 1737-1761, 1971.

VOLLAND, H., A semi-empirical model of large-scale magnetospheric electric fiels, J. Geophys. Res., 78, 171-180, 1973.

VOLLAND, H., Models of global electric fields within the magnetosphere, Ann. Géophys., 31, 159-173, 1975.
VOLLAND, H., A model of the magnetospheric electric convection field, J. Geophys. Res., 83, 2695-2699, 1978.